Optimizing Cylindrical Battery Cooling: Numerical Investigation of a Next-Gen Thermal Architecture

Mohamed Es-satte[1], *Hamza Faraji*[2*], *Ibtissam Afaynou*[1], *Khadija Choukairy*[1], *Imane Regragui*[1] *and Mohamed Bourich*[2]

[1]Laboratory of Computer and Mathematical Process Engineering, National School of Applied Sciences, Sultan Moulay Slimane University, Khouribga, Morocco
[2]Cadi Ayyad University, UCA, National School of Applied Sciences, LaRTID Laboratory, Marrakech, Morocco

Abstract. The growing demand for high-performance lithium-ion (Li-ion) batteries in electric vehicles and portable electronics necessitates efficient thermal management solutions. This study numerically investigates a novel battery thermal management system (BTMS) that integrates aluminum fins with secondary branches embedded in a phase change material (PCM). The influence of the number of secondary fins on the thermal response of the system during battery discharge is analyzed using the enthalpy–porosity method. Results show that the introduction of secondary fins significantly reduces the maximum battery surface temperature by enhancing heat conduction and promoting more uniform heat distribution within the PCM. However, the increased fin density leads to slower PCM melting, as the higher metallic volume reduces the amount of PCM and stores part of the heat through sensible conduction. Consequently, the overall fusion process is delayed, although temperature uniformity is improved. The configuration with two secondary fins per branch provides the best compromise between temperature reduction, melting efficiency, and material usage, making it a promising passive cooling approach for Li-ion battery systems.

Keywords. Battery Thermal Management System, Phase Change Material, Fins, Lithium-ion battery, CFD simulation.

1 Introduction

The rapid expansion of lithium-ion (Li-ion) batteries in electric vehicles has intensified the demand for efficient and reliable thermal management systems. Battery life, performance, and safety deteriorate significantly when cells operate outside their optimal temperature range, and excessive heat generation during fast charge or discharge can even trigger thermal runaway [1].

Phase change materials (PCMs) offer an attractive passive thermal management solution due to their high latent heat capacity, which enables them to absorb substantial amounts of heat at nearly constant temperature. This mechanism effectively moderates temperature rise during transient high-power operation. However, the intrinsically low thermal conductivity of most PCMs restricts their ability to transfer heat away from local hot spots, resulting in sluggish melting and uneven temperature distributions in practical battery configurations [2,3].

* Corresponding author: hamza.faraji@uca.ac.ma

To overcome this limitation, numerous studies have introduced high-conductivity components such as metallic fins, foams, and carbon-based fillers into the PCM matrix, thereby establishing efficient conduction pathways between the heat source and the PCM bulk. Ping et al. [4] demonstrated that the incorporation of properly designed fins can significantly reduce peak cell temperatures and accelerate heat diffusion. Nonetheless, fin geometry and distribution introduce critical trade-offs: while increasing metallic content enhances heat conduction, it simultaneously reduces PCM volume and, consequently, its latent heat storage capacity. Moreover, excessively dense fin arrays can cause overlapping thermal fields and diminishing performance returns.

Liu et al. [5] reported that advanced fin configurations including spiral, honeycomb, and topology-optimized designs can enlarge the effective surface area and direct the melting front more efficiently, while minimizing PCM displacement. Numerical investigations employing ANSYS Fluent and the transient enthalpy–porosity approach have proven effective in analyzing such complex fin geometries, capturing both conductive and convective heat transfer processes within the melting PCM.

Tian et al. [6] further highlighted that biomimetic branching structures inspired by leaf veins and other natural networks represent a promising direction for achieving uniform thermal distribution. These bionic designs facilitate radial and hierarchical heat transfer, enhancing melting uniformity and improving overall thermal safety in battery modules. Several recent works confirm that leaf-vein and self-similar fin structures can markedly improve temperature uniformity and reduce peak temperatures in high-power Li-ion cells.

Despite these advances, the optimal balance between fin density (i.e., the number of secondary branches), PCM utilization (latent heat storage), and long-term thermal response under cyclic operation remains unclear. Specifically, the effect of secondary fin count on both the battery surface temperature and the transient liquid fraction of the PCM has not been comprehensively characterized under realistic discharge powers and geometric constraints. Addressing this gap is essential for developing lightweight, manufactural battery thermal management systems (BTMS) that optimize both safety and energy storage efficiency [7,8].

In this study, a fin-enhanced PCM-based BTMS is investigated, where aluminum primary fins are complemented by a variable number of secondary fins arranged radially around a cylindrical Li-ion cell. Transient simulations using the enthalpy–porosity method are performed to resolve the coupled melting dynamics and conjugate heat transfer between the battery, fins, and PCM. The results quantify the influence of secondary fin number on the battery surface temperature, PCM liquid fraction evolution, and the trade-off between enhanced heat conduction and reduced PCM latent capacity, thereby offering practical guidance for passive cooling system design.

2 Numerical Model and Methodology

2.1 Physical Model Description

The investigated system consists of a single cylindrical Li-ion battery surrounded by a phase change material (PCM) and a set of aluminum fins designed to enhance heat transfer. The fins include secondary branches distributed symmetrically along the main fins, forming a biomimetic pattern inspired by natural leaf veins. The entire structure is enclosed in a casing subject to natural convection with a convection coefficient of 5.7 W/m^2K. No forced airflow or liquid cooling is applied, as the system relies entirely on passive heat dissipation through the PCM and the aluminum fins.

The battery is assumed to generate heat uniformly during the discharge process, and the PCM undergoes a solid–liquid phase transition as it absorbs the released heat. The aluminum fins serve as thermal bridges, facilitating heat conduction from the battery surface to the PCM region, thereby accelerating the melting process.
Table 1 presents the thermophysical properties of the materials employed in this study. Figure 1 shows the proposed BTMS design. To evaluate and compare the performance of various fin configurations, two different fin designs, illustrated in Fig. 2, are examined in this study.

Table 1. Thermo-physical properties of all utilized materials in the present study [9,10].

	PCM		Lithium	Aluminum
	Solid	Liquid		
Density, Kg/m3	910	769	2720	2719
Specific heat capacity, J/kg.K	1926	2400	300	871
Thermal conductivity, W/m.K	0.423	0.146	3	202.4
Melting point, K	309.55	-	-	-
Latent heat of fusion, kJ/kg	248	-	-	-

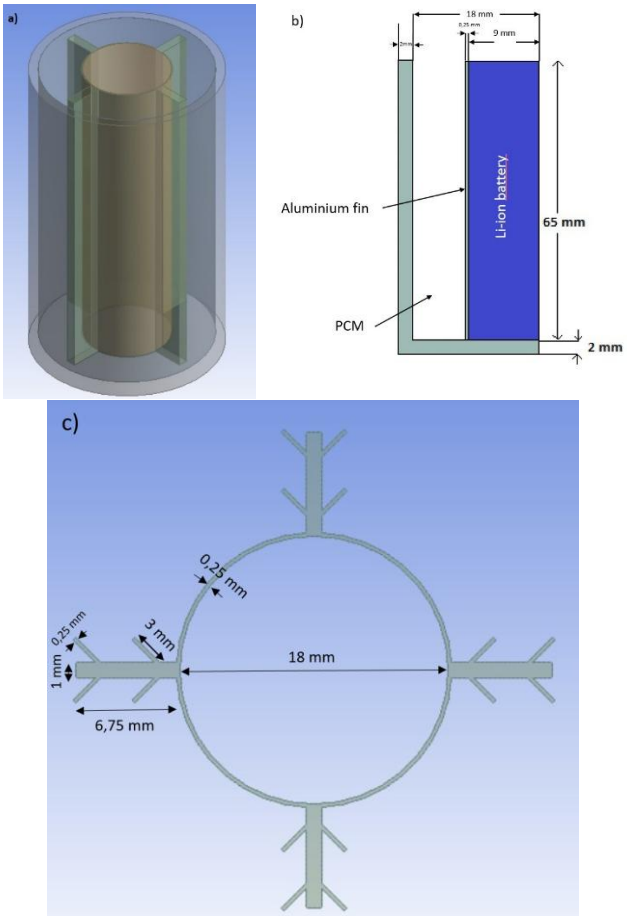

Fig. 1. The proposed BTMS. (a) Three-dimensional model; (b) 2D model viewed along the (y–z) plane; (c) Top view of the model.

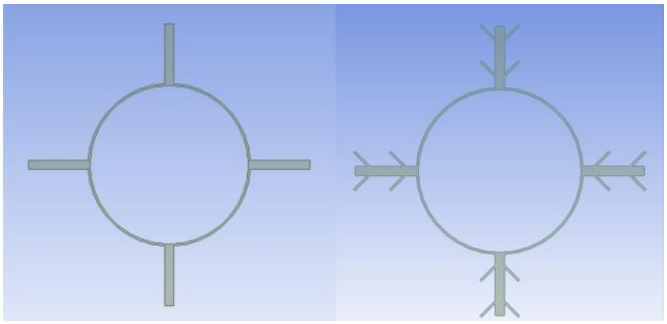

Fig. 2. Various fin configurations examined in this study.

2.2 Governing Equations

The heat transfer within the battery, aluminum fins, and PCM domain is described by the transient heat conduction equation. For the PCM, the phase change process is modeled using the enthalpy–porosity method [11], which accounts for the latent heat during melting:

$$\rho \frac{\partial H}{\partial t} = \nabla . (k \nabla T) \tag{1}$$

where ρ is the density, k is the thermal conductivity, T is the temperature, and h is the specific enthalpy defined as:

$$H = H_{ref} + \int_{T_{ref}}^{T} c_p dT + f_l L \tag{2}$$

Here, C_p is the specific heat capacity, L is the latent heat of fusion, H_{ref} is the reference specific enthalpy, and f_l is the liquid fraction, expressed as:

$$f_l = \begin{cases} 0, & T < T_{solidus} \\ \frac{T - T_{solidus}}{T_{liquidus} - T_{solidus}}, & T_{solidus} \le T \le T_{liquidus} \\ 1, & T > T_{liquidus} \end{cases} \tag{3}$$

2.3 Boundary and Initial Conditions

Initial Condition: The entire domain is initially at a uniform temperature $T_0 = 305\ K$, below the PCM melting point.

$$T(x, y, t = 0) = T_0 \tag{4}$$

Battery Surface: A constant heat flux q is applied to represent the heat generated during battery discharge:

$$-k \frac{\partial T}{\partial n} = q \tag{5}$$

External Boundaries: The outer surface of the enclosure was exposed to ambient air and subjected to natural convective heat transfer, described by the following boundary condition:

$$-k\frac{\partial T}{\partial n} = h(T_s - T_\infty) \tag{6}$$

Where k is the thermal conductivity of the wall material, T_s is the surface temperature, T_∞ is the ambient air temperature, and h is the convective heat transfer coefficient. In this study, a value of h=5.7 W/m^{2}K was used to represent natural air convection around the BTMS module, while the ambient temperature was fixed at T_∞=305 K

Interface Conditions: At the interfaces between the battery, fins, and PCM, temperature and heat flux are continuous:

$$T_{PCM} = T_{fin} = T_{battery} \tag{7}$$

$$k_{PCM}\frac{\partial T}{\partial n} = k_{fin}\frac{\partial T}{\partial n} \tag{8}$$

2.4 Numerical Procedure

The numerical simulation is carried out using ANSYS Fluent, employing the finite volume method to discretize the governing equations. The enthalpy–porosity formulation is used to capture the melting front evolution within the PCM. The computational mesh is refined near the battery surface and around the fin–PCM interfaces to accurately resolve temperature gradients.

A grid independence study is performed to ensure mesh quality and solution accuracy. Time-step sensitivity is also checked to ensure temporal stability. Convergence is assumed when the residuals of energy equations fall below 10^{-6} and the temperature variation between successive iterations is less than 10^{-5}.

3 Numerical model validation

3.1 Mesh and time step independent test

The numerical model described in this study was implemented to solve the governing equations of heat transfer and phase change within the battery thermal management system. The computations were performed using the finite volume method available in ANSYS Fluent 19.2. The SIMPLE algorithm was employed to couple the pressure and velocity fields, ensuring numerical stability and accuracy. A second-order upwind scheme was applied for the discretization of momentum, energy, and scalar transport equations, whereas the PRESTO! scheme was utilized for pressure interpolation. To accelerate convergence and maintain stability, the under-relaxation factors for density, pressure, liquid fraction, momentum, and energy were set to 1.0, 0.3, 0.9, 0.5, and 0.9, respectively. The solution was considered converged when the residuals of the continuity, momentum, and energy equations dropped below 10^{-3}, 10^{-5}, and 10^{-8}, respectively.
A preliminary sensitivity analysis was carried out to evaluate the influence of grid resolution and time-step size on the numerical accuracy. Three grid configurations (1.2, 1.0 and 0.8 mm) and three-time steps (1, 0.5, and 0.25 seconds) were examined. The assessment focused

on the melting behaviour of pure n-eicosane, tracking both the liquid fraction and the peak temperature of the surface cell.
According to the results summarized in Table 2 and Table 3 at t = 1500 s, refining the mesh from 1 mm to 0.8 mm with a time step of 1s produces only slight variations, about 0.56% in the liquid fraction and 0.19% in the maximum surface cell temperature. Similarly, reducing the time step from 0.5s to 0.25s results in negligible changes of approximately 0.24% and 0.11%, respectively. These findings indicate that the mesh size of 1 mm and a time step of 0.5 s provide an optimal balance between computational efficiency and solution accuracy.

Table 2. Dependence on grid size at t = 1500s

mesh size	number of elements	Liquid fraction	Deviation (%)	Temperature	Deviation (%)
1,2 mm	179402	0,0856	-	316,38	-
1 mm	322807	0,0876	2,28	315,62	0,24
0,8 mm	602884	0,0881	0,56	315,01	0,19

Table 3. Dependence on time step at t = 1500s

Time step (s)	Liquid fraction	Deviation (%)	Temperature	Deviation (%)
1s	0,0785	-	315	-
0,5s	0,0823	4,61	315,33	0,10
0,25s	0,0825	0,24	315,7	0,11

3.2 Validation of the numerical model

To assess the reliability of the numerical methods employed for simulating PCM melting and heat transfer, the predicted temperature profile was compared with previously reported experimental results. The numerical predictions were also confronted with available experimental data and earlier numerical study conducted by Zheng et al. [10], as presented in Fig. 3. The comparison indicates that the present simulations show good agreement with the reference data.

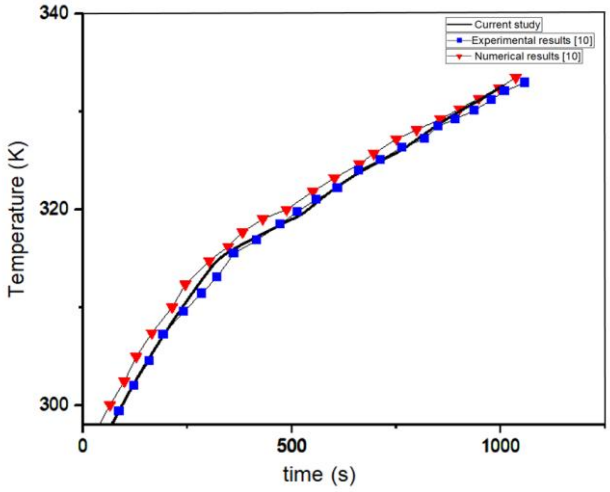

Fig. 3. Variations with time of the battery surface temperature.

4 Results and discussion

4.1 Temperature evolution and isotherm fields

To evaluate the thermal performance of the proposed BTMS configurations, Fig. 4 presents the temporal evolution of the battery surface temperature for the three investigated configurations: pure PCM, primary fins only, and fin systems enhanced with two secondary branches. As expected, the configuration without fins exhibits the highest and fastest temperature rise, reaching more than 330 K, which clearly demonstrates the inability of the PCM alone to dissipate heat efficiently during continuous discharge. The introduction of aluminum fins markedly improves heat spreading inside the PCM, reducing the peak temperature by more than 20 K relative to the PCM-only case.
Increasing the number of secondary branches further improves thermal regulation. The configuration with secondary branches shows a moderate reduction in surface temperature compared to simple radial fins. This improvement is attributed to the enhanced conductive pathways created by the secondary branches, which distribute heat more uniformly and accelerate its transfer from the battery to the surrounding PCM.

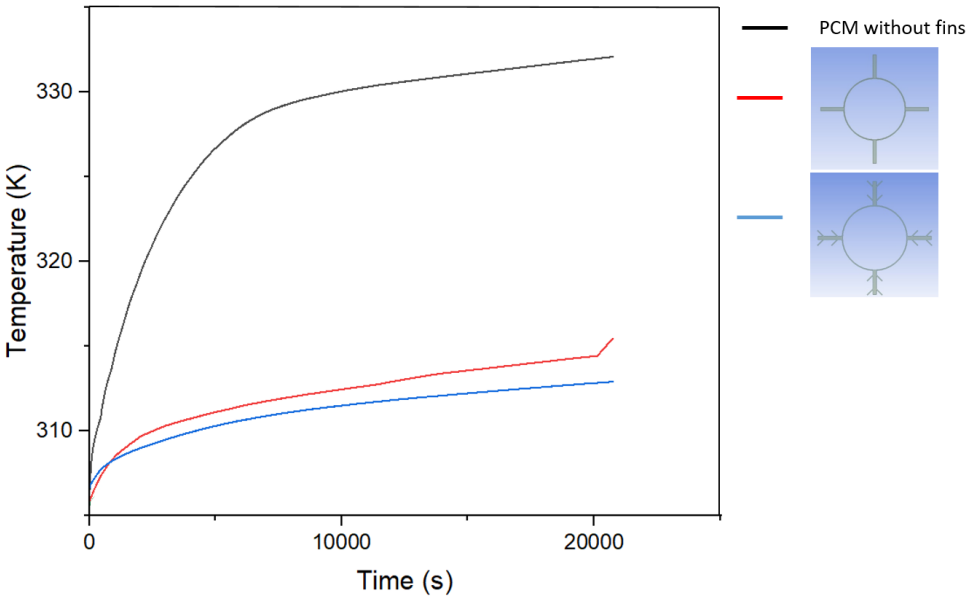

Fig. 4. Time-dependent evolution of the surface cell temperature for the three investigated cases.

Fig. 5 presents the evolution of isotherms at different instants. The comparison of the three configurations highlights the dominant influence of fin geometry on heat spreading within the PCM-based BTMS. The baseline case with pure PCM exhibits radially symmetric isotherms and a pronounced central hot zone, confirming that conduction through the PCM alone is insufficient to dissipate the imposed heat load.
The introduction of simple fins significantly modifies the thermal field by establishing preferential conduction paths. The resulting anisotropic isotherm structure and reduction in core temperature demonstrate an improved extraction of heat toward the boundaries, although heat transfer remains strongly direction-dependent.

Branched fin configurations further enhance thermal homogenization. The addition of secondary branches increases the effective conductive interface with the PCM, producing a measurable reduction in spatial gradients.

These results underline a key design trade-off: increasing fin complexity improves conduction but reduces PCM volume and latent heat capacity. The two-branch configuration offers the most favorable balance, providing a substantial improvement in temperature uniformity without excessive geometric complexity or significant loss of storage material.

Overall, the study confirms that optimally branched fin networks can significantly improve BTMS thermal performance, but their design must consider conduction enhancement, PCM volume reduction, and manufacturability simultaneously. Further quantitative assessment of thermal resistance, melt fraction, and stored energy will refine this optimization.

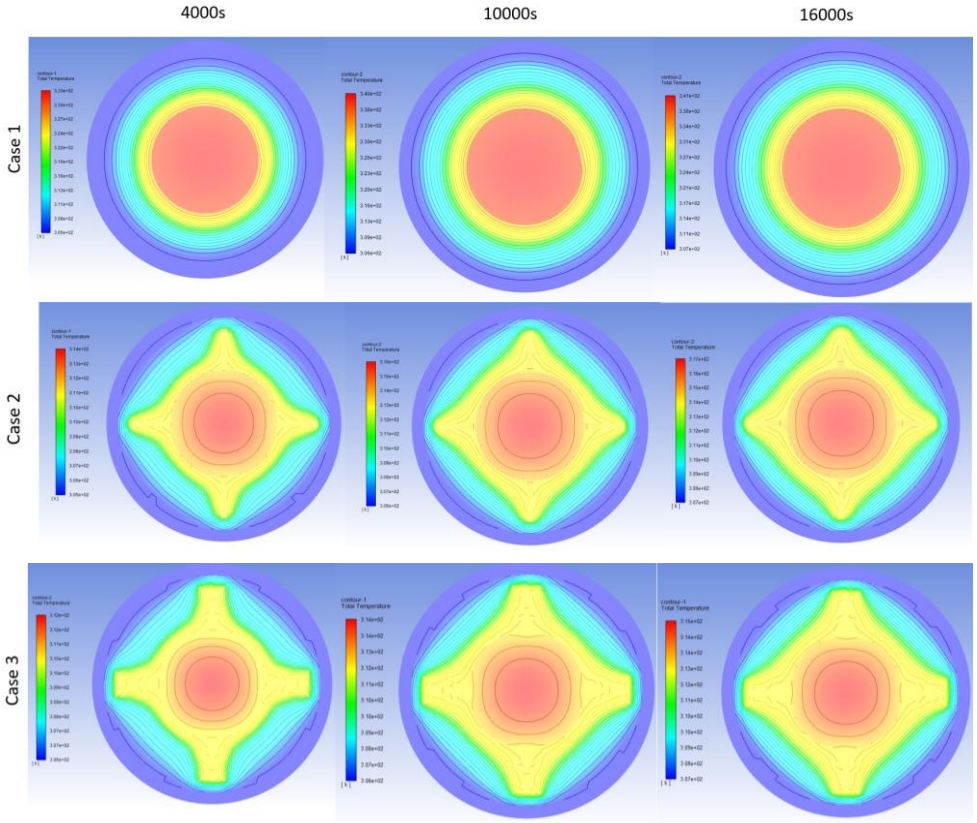

Fig. 5. Evolution of isotherm contours for the three cases.

4.2 Liquid fraction evolution and melting dynamics

Fig. 6 illustrates the PCM liquid fraction variations with different cases. The pure PCM melts significantly faster due to localized overheating near the battery surface, which triggers early melting but with poor spatial uniformity. The finned configurations exhibit slower and more gradual melting: improved conduction spreads heat over a larger PCM volume, delaying the onset of local full melting. Increasing the number of branches slows the overall melt rate even further, an effect that arises from stronger heat diffusion through the metallic network, which lowers local temperatures within the PCM and stabilizes the melting front. This behavior highlights a key trade-off: although additional secondary fins reduce PCM melting rate, they substantially enhance battery-cooling performance.

The spatial distributions of liquid fraction (Figure 7) provide deeper insight into this behavior. In the simple-fin configuration, melting initiates primarily along the main fin axes and forms an elongated melt region. In contrast, the branching configurations promote a more radially symmetric melting pattern with reduced thermal gradients. The two-level design achieves the most homogeneous temperature field, effectively suppressing hot spots around the battery casing. These results confirm the ability of branching fin networks to guide both heat and melt propagation in a controlled manner.

Overall, the results demonstrate that integrating secondary fin structures significantly enhances thermal performance by lowering the peak battery temperature, homogenizing heat distribution, and stabilizing PCM melting dynamics.

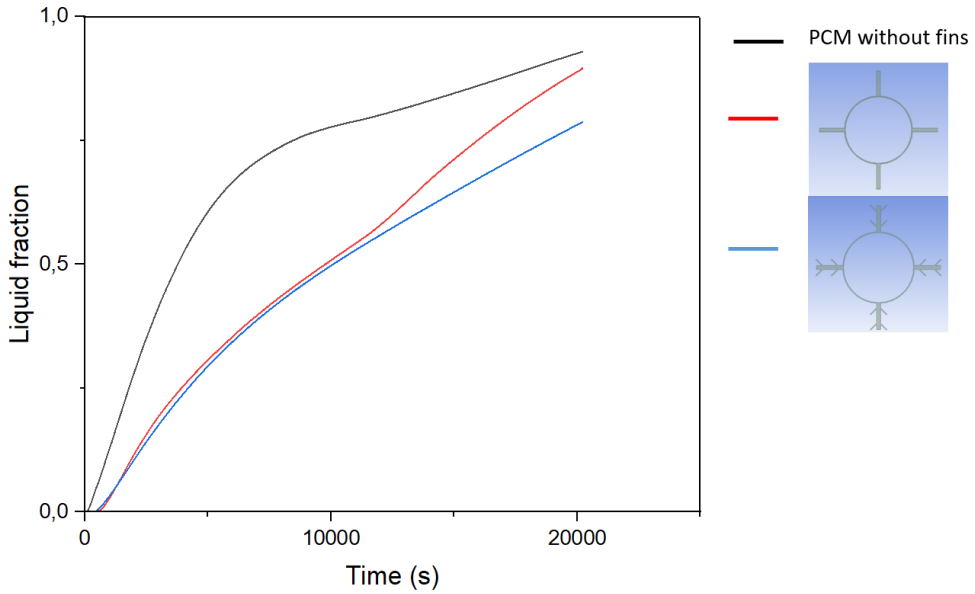

Fig. 6. PCM liquid fraction variations with different cases.

Fig. 7 presents the liquid fraction distribution at different instants. The analysis of the liquid fraction distribution highlights the structural influence of fins on the melting behavior of the PCM.

The incorporation of fins enhances heat spreading toward the core of the system and leads to a more homogeneous temperature field. However, the liquid fraction profiles clearly indicate a noticeable deceleration of the overall melting process when fins are added. This behavior arises from two combined effects: the additional solid mass introduced by the fins, which absorbs a substantial portion of the heat input before it reaches the PCM, and the attenuation of local temperature gradients in the vicinity of the conductive fin surfaces, which limits the advancement speed of the solid–liquid interface.

Despite this slowdown, the configuration employing branched secondary fins exhibits a more uniform melting front and deeper thermal penetration into the PCM, effectively mitigating the under-heated regions observed in the other cases. This design thus improves the overall thermal effectiveness of the BTMS, although the melting rate remains lower than that of the fin-free configuration.

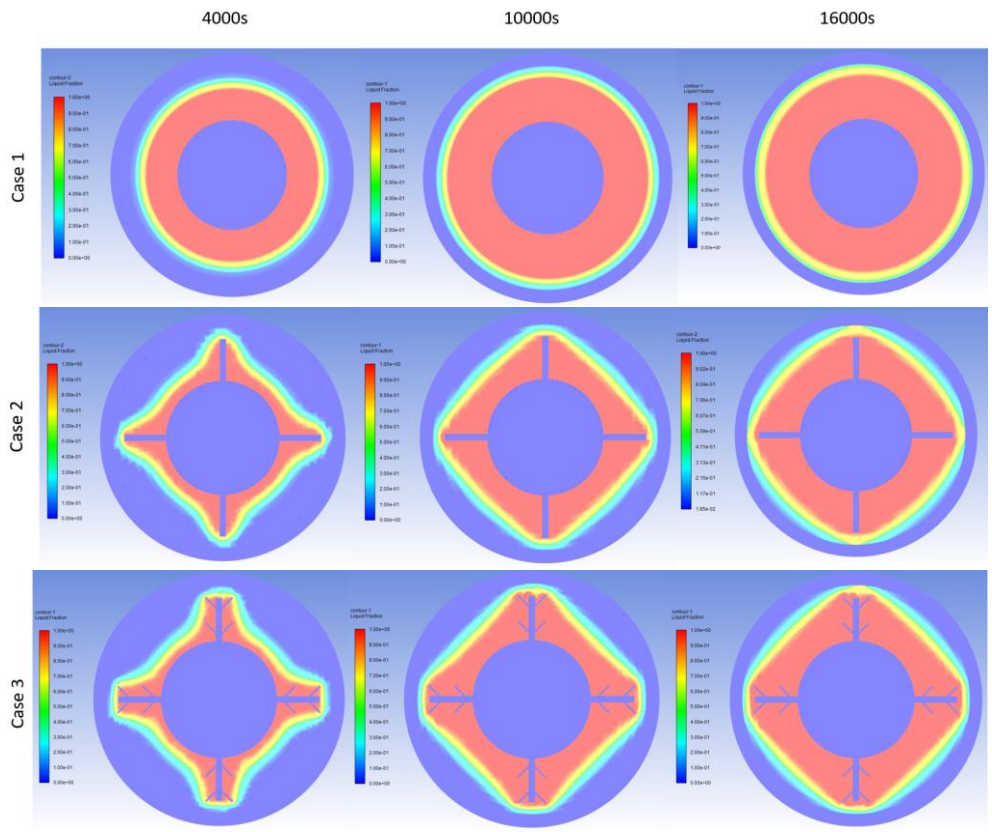

Fig. 7. Liquid fraction distribution at different instants.

5 Conclusion

This study numerically evaluated the thermal behavior of a cylindrical Li-ion battery embedded in PCM and enhanced with aluminum fins. The results demonstrate that while PCM alone cannot prevent battery overheating, the integration of fins substantially improves heat spreading and reduces peak temperatures. Adding secondary branches enhances thermal uniformity but slows melting due to increased solid mass and reduced PCM volume. Among all configurations, the two-level branching design offers the best compromise between conductive enhancement and latent-heat utilization, achieving the lowest battery surface temperature and the most homogeneous thermal field while maintaining a larger amount of PCM compared to the other design. These findings provide practical guidance for designing high-performance, lightweight, and manufactural passive BTMS for next-generation cylindrical Li-ion batteries.

References

[1] K. Jiang, G. Liao, J. E, F. Zhang, J. Chen, E. Leng, Thermal management technology of power lithium-ion batteries based on the phase transition of materials: A review, J. Energy Storage 32 (2020) 101816. https://doi.org/10.1016/j.est.2020.101816.

[2] J. Luo, D. Zou, Y. Wang, S. Wang, L. Huang, Battery thermal management systems (BTMs) based on phase change material (PCM): A comprehensive review, Chem. Eng. J. 430 (2022) 132741. https://doi.org/10.1016/j.cej.2021.132741.

[3] M. Es-satte, I. Afaynou, H. Faraji, K. Choukairy, I. Regragui, K. Amghar, M. Boucetta, S. Saadeddine, M. Bourich, Phase change materials, bionic structures and artificial intelligence for lithium-ion battery thermal management: A comprehensive review, Int. Commun. Heat Mass Transf. 173 (2026) 110870. https://doi.org/10.1016/j.icheatmasstransfer.2026.110870.

[4] P. Ping, R. Peng, D. Kong, G. Chen, J. Wen, Investigation on thermal management performance of PCM-fin structure for Li-ion battery module in high-temperature environment, Energy Convers. Manag. 176 (2018) 131–146. https://doi.org/10.1016/j.enconman.2018.09.025.

[5] J. Liu, Q. Ma, X. Li, Numerical Simulation of the Combination of Novel Spiral Fin and Phase Change Material for Cylindrical Lithium-Ion Batteries in Passive Thermal Management, Energies 15 (2022) 8847. https://doi.org/10.3390/en15238847.

[6] Y. Tian, M. Ji, X. Qin, C. Yang, X. Liu, Self-growing bionic leaf-vein fins for high-power-density and high-efficiency latent heat thermal energy storage, Energy 309 (2024) 133086. https://doi.org/10.1016/j.energy.2024.133086.

[7] V. Saxena, S.K. Sahu, S.I. Kundalwal, P.A. Tsai, Optimizing battery thermal management with phase change materials: Influence of thickness, ambient conditions, and material selection, J. Energy Storage 132 (2025) 117657. https://doi.org/10.1016/j.est.2025.117657.

[8] S.I. Alma'asfa, M.S. Abdul Aziz, C.Y. Khor, F.Y. Fraige, Thermal management of cylindrical lithium-ion batteries with different fin configurations and phase change material: a numerical analysis, J. Therm. Anal. Calorim. 150 (2025) 12643–12662. https://doi.org/10.1007/s10973-025-14515-y.

[9] M.D. Muhammad, O. Badr, H. Yeung, Validation of a CFD Melting and Solidification Model for Phase Change in Vertical Cylinders, Numer. Heat Transf. Part Appl. 68 (2015) 501–511. https://doi.org/10.1080/10407782.2014.994432.

[10] H. Najafi Khaboshan, F. Jaliliantabar, A. Adam Abdullah, S. Panchal, Improving the cooling performance of cylindrical lithium-ion battery using three passive methods in a battery thermal management system, Appl. Therm. Eng. 227 (2023) 120320. https://doi.org/10.1016/j.applthermaleng.2023.120320.

[11] H. Najafi Khaboshan, F. Jaliliantabar, A.A. Abdullah, S. Panchal, A. Azarinia, Parametric investigation of battery thermal management system with phase change material, metal foam, and fins; utilizing CFD and ANN models, Appl. Therm. Eng. 247 (2024) 123080. https://doi.org/10.1016/j.applthermaleng.2024.123080.